Biosensors and Bioelectronics 42 (2013) 321–325

Contents lists available at SciVerse ScienceDirect

Biosensors and Bioelectronics

journal homepage: www.elsevier.com/locate/bios

Short communication

An electrochemical biosensor based on human serum albumin/graphene oxide/3-aminopropyltriethoxysilane modified ITO electrode for the enantioselective discrimination of D- and L-tryptophan

Erhan Zor [a], Imren Hatay Patir [b,*], Haluk Bingol [c], Mustafa Ersoz [b]

[a] Selcuk University, Science Institute, 42003 Selcuklu/Konya, Turkey
[b] Selcuk University, Science Faculty, Chemistry Department, 42031 Selcuklu/Konya, Turkey
[c] Necmettin Erbakan University, Ahmet Kelesoglu Education Faculty, Chemistry Department, 42099 Meram/Konya, Turkey

ARTICLE INFO

Article history:
Received 11 October 2012
Accepted 21 October 2012
Available online 2 November 2012

Keywords:
Chiral sensor
Enantioselectivity
Indium tin oxide
Graphene oxide
Tryptophan
Human serum albumin

ABSTRACT

A new electrochemical biosensor based on the human serum albumin/graphene oxide/3-aminopropyltriethoxysilane modified indium tin oxide electrode (ITO/APTES/GO/HSA) has been developed for the discrimination of tryptophan (Trp) enantiomers. The electrode has been characterized by scanning electron microscopy (SEM) and electrochemical techniques. The electrochemical behaviors of the enantiomeric pairs (D- and L-Trp) at the ITO/APTES/GO/HSA electrode have been investigated by cyclic voltammetry in the concentration range of 0.10–1.0 mM. A clear separation between the oxidation peak potentials of D- and L-Trp, at 0.86 and 1.26 V, respectively, has suggested that the ITO/APTES/GO/HSA electrode can be used as an electrochemical biosensor for the discrimination of Trp enantiomers. In order to find the percentage of an enantiomeric form of tryptophan in a mixture, the ITO/APTES/GO/HSA electrode is used for the simultaneous detection of D- and L-Trp which showed that the percentage of one enantiomeric form can be easily measured in the presence of the other.

1. Introduction

Enantioselective discrimination of chiral biologically active synthetic and natural compounds is a fundamental area with increasing importance in chemical, clinical, food and pharmaceutical industry due to their vital importance in living systems (Xuan et al., 2012; Girardet et al., 2007; Chen et al., 2012). Numerous compounds are known to be a racemic mixture of enantiomers. One enantiomer may influence desirable property while the other may be ineffective or often exhibits a different physiological role and may cause serious side-effects (Izake, 2007; Zhao et al., 2008; Bu et al., 2012). For instance, among amino acids, tryptophan (Trp) is an essential constituent of proteins and precursor of melatonin (a neurohormone) and serotonin (a neurotransmitter) which improve the sleep, mood and mental health (Guo et al., 2010; Mazloum-Ardakani et al., 2010; Özcan and Sahin, 2012). Due to importance of enantiomeric purity (Trojanowicz and Wcisło, 2005), the enantioselective discrimination of Trp enantiomers has become extraordinarily important and many efforts have been paid for discrimination of enantiomers of Trp.

Various techniques have been developed such as the fluorometric micromethod (Miller et al., 1956), capillary electrophoresis (Simionato et al., 2008), high performance liquid chromatography (Zhen et al., 2011), chemoluminescence (Liang and Song, 2005) and the electrochemical method (Bu et al., 2012) for enantiomeric determination of Trp. Although the reported techniques are useful for the determination of enantiomeric purity, these are not only time-consuming and need expensive equipments but also many of them have indicated no difference between two enantiomeric forms of Trp. In this context, electrochemical methods have been one of the widely used methods for the detection of enantiomers owing to their advantages in ease of preparation, accuracy, low material cost, high stability and sensitivity (Xu et al., 2012).

Graphene-based materials have been one of the fascinating applications in electrochemical sensors and biosensors, which provide an effective sensing platform for small biomolecules (Wang et al., in press). Usually, working with modified forms of graphene begins with chemically oxidized graphene oxide (GO) in sensor applications. GO based materials with tunable oxygen functionalities on their basal planes facilitate the surface modification with other materials (Kumar et al., 2012).

The aim of this work is to fabricate a novel and stable graphene oxide-based electrochemical biosensor for the discrimination of

* Corresponding author. Tel.: +90 3322233898; fax: +90 3322412499.
E-mail addresses: zorerhan@gmail.com (E. Zor), imrenhatay@gmail.com (I. Hatay Patir), halukbingol@gmail.com (H. Bingol), ersozm@gmail.com (M. Ersoz).

0956-5663/$ - see front matter © 2012 Elsevier B.V. All rights reserved.
http://dx.doi.org/10.1016/j.bios.2012.10.068

two enantiomeric forms of Trp. ITO electrode surface has been firstly modified with APTES (ITO/APTES) then further with GO (ITO/APTES/GO) and finally with HSA (ITO/APTES/GO/HSA). The electrochemical behaviors of D- and L-Trp at the ITO/APTES/GO/HSA electrode have been analyzed by cyclic voltammetry (CV). The voltammetric results indicate that two enantiomers of Trp can be easily and remarkably discriminated by the ITO/APTES/GO/HSA electrode. In addition, the enantiomeric percentage of D- and L- Trp has been successfully determined. The results show that the ITO/APTES/GO/HSA can be used as an effective tool to discriminate Trp in electrochemical biosensor applications. While there are some reports on the electrochemical detection of Trp (Jiang et al., 2010; Raoof et al., 2009; Prabhu et al., 2011), to the best of our knowledge there is no prior report on the electrochemical detection and, in particular, the enantioselective discrimination of L- and D-Trp by CV technique.

2. Experimental

Full chemical and apparatus details and analytical data can be found in the Supporting Information (SI).

2.1. Preparation of graphene oxide

Graphene oxide (GO) was synthesized from graphite powder by the improved method (Marcano et al., 2010), which has significant advantages over Hummers' method (Hummers and Offeman, 1958), with an additional preoxidation process. The synthesis procedure and the resulting XRD pattern (Fig. SI1) were given in SI.

2.2. Preparation of modified electrodes

ITO electrodes were precleaned with acetone, ethanol and a copious amount of deionized water. The electrodes were then treated in a solution of $H_2O_2/NH_4OH/H_2O$ (1:1:5) for 30 min at 60 °C to obtain hydroxylated active ITO surface. The activated ITO glass plates were immersed 2.0% APTES solution prepared in toluene at 70 °C for 48 h (Kim et al., 2004). The ITO/APTES electrodes were then rinsed with toluene (3 times) to remove non-bonded silane molecules from the glass surface and dried under N_2. After rinsing with ethanol and drying under N_2 atmosphere, the APTES-modified ITO electrodes were immersed in a suspension of GO (0.2 mg/mL) for 5 h to obtain APTES/GO-modified ITO electrode surface. After rinsing with ultra-pure water and drying under N_2 atmosphere the electrodes obtained were immersed in a phosphate buffer containing HSA (10 mg/mL, pH 7.4) for 12 h at about +4 °C in order to prepare the APTES/GO/HSA-modified ITO electrodes. The APTES/GO/HSA-modified ITO electrodes were then washed with ultra-pure water and dried under N_2 before use. The ITO/APTES/GO/HSA electrode was stored in a phosphate buffer at about +4 °C in a closed vessel when not in use.

3. Results and discussion

3.1. Electrochemical characterization of modified electrodes by CV and EIS

As shown in Fig. 1, a peak-to-peak potential difference (ΔE_p) and peak-to-peak current difference (ΔI_p) of the $[Fe(CN)_6^{-3/-4}]$ redox couple show the changes at each step of the surface modification of ITO. The bare ITO shows a quasi-reversible electrochemical response for the $[Fe(CN)_6^{-3/-4}]$ redox couple with ΔE_p of 285 mV and ΔI_p of 0.48 mA. The modification of ITO surface with APTES presents an increased ΔI_p of 0.63 mA and a decreased ΔE_p of 235 mV. This result is attributed that a positively charged amino group of the APTES molecule which get protonated (NH_3^+) in aqueous solution attracts the negative charge of $[Fe(CN)_6^{-3/-4}]$, causing an easy electron transfer reaction on the electrode surface (Haak et al., 2010). Cyclic voltammogram of ITO/APTES/GO electrode shows similar peak-to-peak potential separation to that of ITO/APTES (ΔE_p=232 mV) but ΔI_p value of ITO/APTES electrode decreases from 0.63 mA to 0.37 mA after GO modification. As reported previously, the reason is explained that GO is negatively charged in solution due to the ionized functional groups such as epoxy, hydroxyl and carboxyl which generate a repulsive interaction with anionic redox probe $[Fe(CN)_6^{-3/-4}]$ (Wang et al., 2009). Further, HSA modification on ITO/APTES/GO electrode surface gives rise to a significant change on the electrochemical behavior of the $[Fe(CN)_6^{-3/-4}]$ couple, leading to strongly increased ΔE_p of 380 mV and decreased ΔI_p value of 0.19 mA. HSA molecule, which is modified on the ITO/APTES/GO electrode through the hydrophobic or electrostatic/hydrogen bonding interactions between GO and HSA, causes the blockage of the electrode surface for oxidation/reduction of the redox probe ($[Fe(CN)_6^{-3/-4}]$) (Heli et al., 2007).

The impedance values are fitted to standard Randle's equivalent circuit (Fig. SI2) which comprises the Ohmic resistance of the electrolyte solution (R_s), surface double-layer capacitance (C_{dl}), Warburg impedance (Z_w) and charge transfer resistance (R_{ct}) as shown in the inset of Fig. 1 (see also Fig. SI3). The bare ITO electrode shows a low frequency straight line with a semicircle portion at high frequency region with charge transfer resistance (R_{ct}) of 183 Ω. The functionalization of ITO surface with APTES gives rise to an almost straight line in the impedance plot which is the characteristic of a diffusion-controlled process for the $[Fe(CN)_6^{-3/-4}]$ electron transfer reaction. In this case, the R_{ct} value is dramatically reduced to 38 Ω, pointing out an easy electron transfer to the electrode surface (Ahuja et al., 2010). The modification of GO on the ITO/APTES electrode results in an increase of R_{ct} value to 200 Ω which is close to that of bare ITO electrode indicating that GO modification leads to a small interfacial electron transfer resistance. Indeed, the present data corroborate the work of Wang et al. who studied the detection of DNA with reduced graphene oxide-coated APTES modified glassy carbon electrode (GCE-APTES-rGO) (Wang et al., 2011). The subsequent modification of HSA on the ITO/APTES/GO electrode leads to a considerable increase of the R_{ct} value to 1961 Ω which indicates the blocking effect of the HSA layer.

3.2. Surface characterization of modified electrodes by SEM

The surface morphology of electrodes was elucidated through the use of SEM. The bare ITO simply shows a smooth surface (Fig. 2a). On the other hand, the SEM image of ITO/APTES/GO electrode shows island-like morphology (see Fig. 2b). The modification of HSA molecule on ITO/APTES/GO electrode results in a well coverage of the HSA molecules on the surface as illustrated in Fig. 2c.

3.3. Enantioselective discrimination of D-and L-Trp at ITO/APTES/GO/HSA electrode

A potential response through the enantioselective discrimination of L- and D-Trp has been investigated by CV for each modification step of the bare ITO electrode. The bare ITO shows a polarization window (Fig. SI4) from −0.80 to 0.87 V. Each step of the ITO surface modification leads to extended polarization window. The bare ITO, ITO/APTES electrodes did not show any

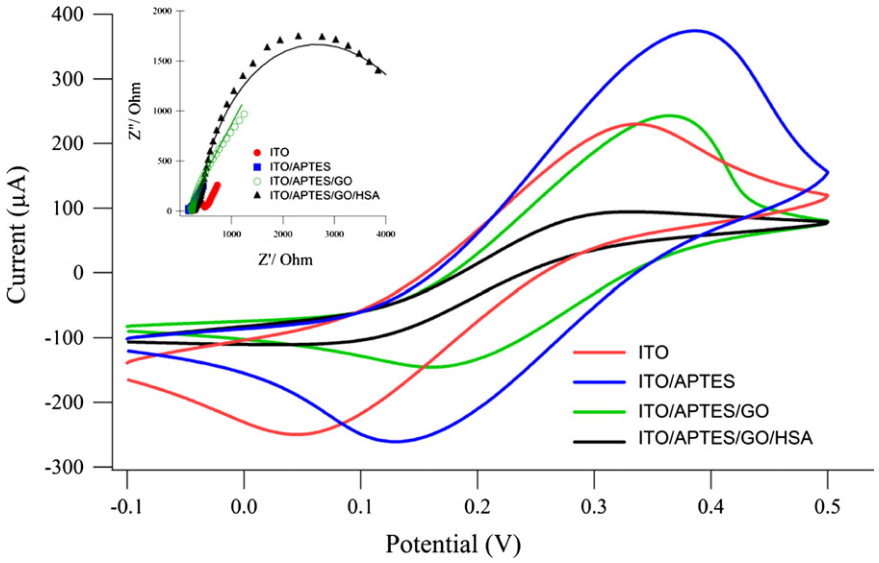

Fig. 1. Cyclic voltammograms obtained 1 mM $[Fe(CN)_6^{-3/-4}]$ redox probe in PBS pH 7.01 at a potential scan rate of 0.1 V s^{-1} for the bare ITO (red line), ITO/APTES (blue line), ITO/APTES/GO (green line), ITO/APTES/GO/HSA (black line) electrodes. Inset: impedance plots (Nyquist plots) obtained for the bare ITO electrode (red circle), ITO/APTES (blue square), ITO/APTES/GO (green hollow circle), ITO/APTES/GO/HSA (black triangle) electrodes. (For interpretation of the references to color in this figure legend, the reader is referred to the web version of this article.)

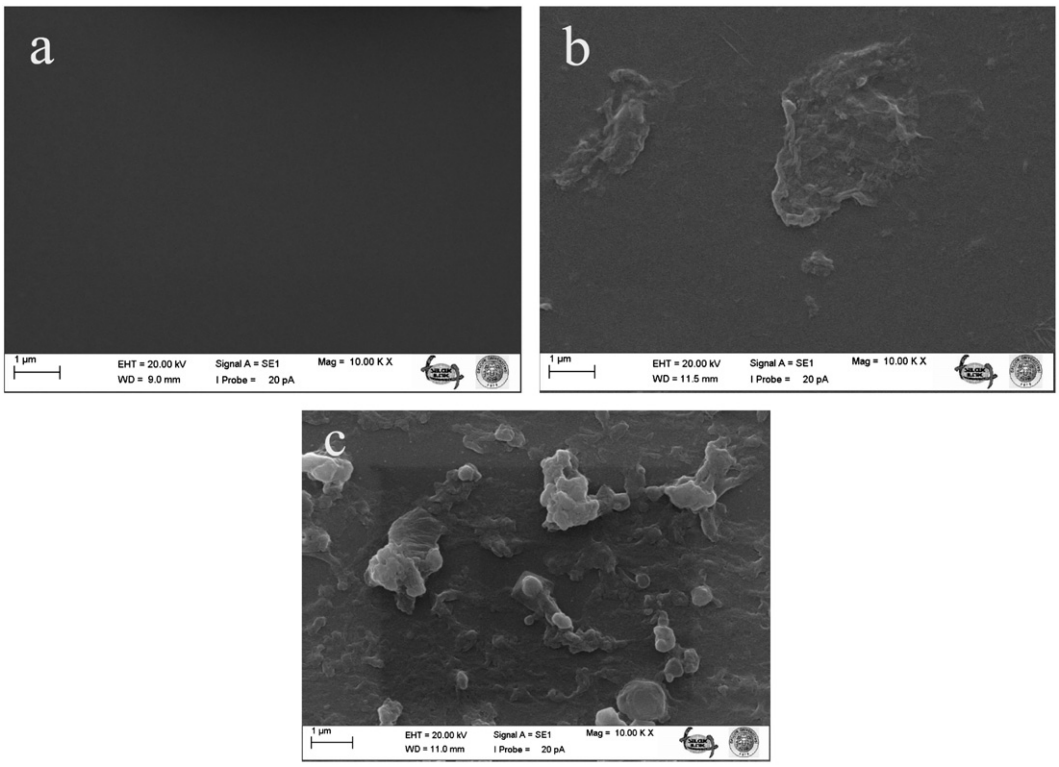

Fig. 2. SEM micrographs of (a) ITO (b) ITO/APTES/GO and (c) ITO/APTES/GO/HSA electrodes.

potential response for the Trp enantiomers within the available polarization window (Figs. SI4-SI5). The ITO/APTES/GO electrode shows only one oxidation peak of about 1.00 V for each enantiomer (D- and L-Trp), indicating no separation of the enantiomeric pairs (Fig. SI6).

The response of an electrochemical sensor in discrimination of enantiomeric pairs can be achieved by the selection of a chiral selector incorporated to the electrode surface on which the interaction of the selector with the analyte is detected. Herein, the discrimination of Trp enantiomers has been studied using HSA which is a well known chiral selector for Trp (Matsunaga et al., 2008). As it can be seen clearly in Fig. 3a, when HSA is modified on ITO/APTES/GO electrode surface, D- and L-Trp enantiomers exhibit well-defined irreversible oxidation peaks at different potential values of 0.86 and 1.26 V, respectively. It has been reported previously that L-Trp interacts more strongly with HSA (Matsunaga et al., 2008). For this reason, the oxidation of L-Trp occurs at more positive potential value. In addition, the potential shift of D-Trp oxidation to a lower value can be attributed to the HSA which acts as a mediator facilitating the electron transfer for

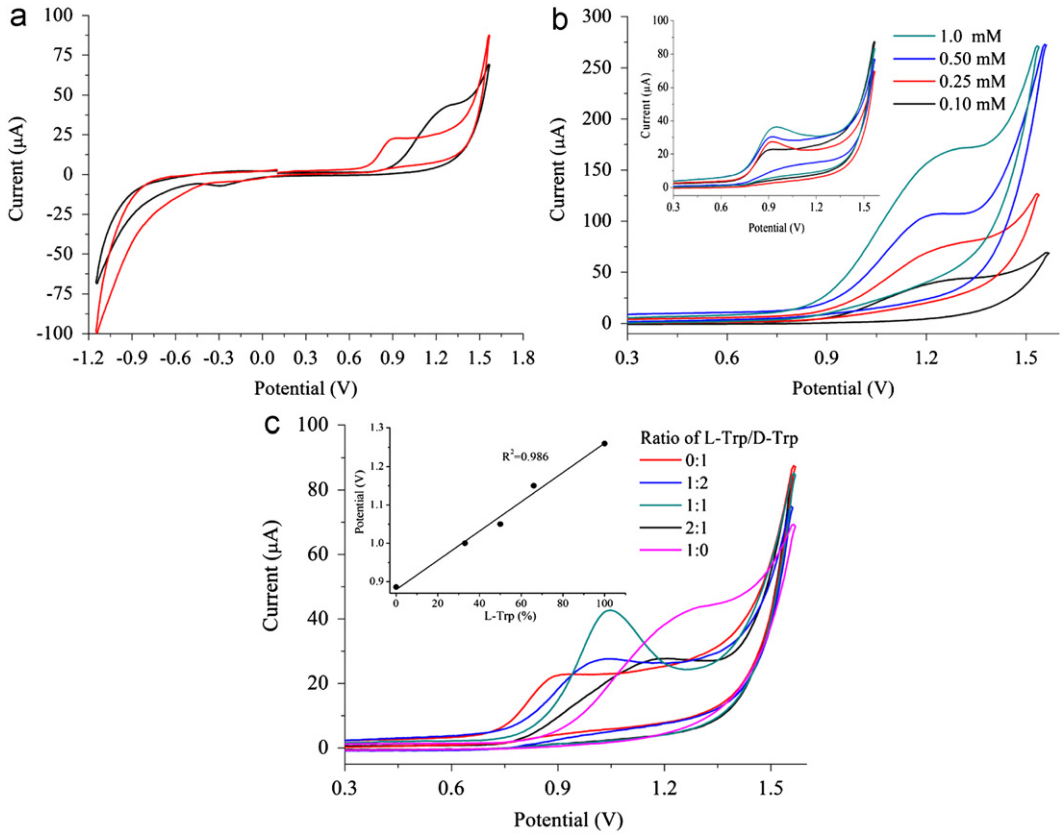

Fig. 3. (a) Cyclic voltammograms of D-Trp (red line) and L-Trp (black line) (0.1 mM) at ITO/APTES/GO/HSA electrode (pH 7.4). Scan rate 0.05 V s^{-1}. (b) Cyclic voltammograms of increasing amount of L-Trp (0.10–1.0 mM) and D-Trp (0.10-1.0 mM) (inset) at ITO/APTES/GO/HSA electrode. Scan rate 0.05 V s^{-1}. (c) Cyclic voltammograms of enantiomeric mixtures of a concentration ratio of L- and D-Trp (1:0 (pink line), 2:1 (black line), 1:1 (green line), 1:2 (blue line) and 0:1 (red line), c/c) at ITO/APTES/GO/HSA electrode. Inset: the linear calibration curve for the percentage of L-Trp versus peak potential value. (For interpretation of the references to color in this figure legend, the reader is referred to the web version of this article.)

oxidation of D-Trp. These results indicate that the ITO/APTES/GO/HSA electrode discriminates the enantiomeric pairs of Trp. It can be attributed to the graphene oxide layer immobilized on the electrode surface that not only provides a large surface for stabilization of HSA at the electrode surface but also separates the analytical signal occurring at the end of the interaction between HSA and D- or L-Trp. A clear separation between oxidation potentials of enantiomeric pairs of Trp depicts that the ITO/APTES/GO/HSA electrode can be used as an electrochemical biosensor for discrimination of Trp enantiomers.

In order to gain an insight to the relationship between the peak current and the concentration of Trp, additional CV measurements were performed in the presence of different concentrations of D-and L-Trp. As shown in Fig. 3b, the oxidation peak current of L-Trp is directly proportional to the concentration increase of L-Trp in the range of 0.10–1.0 mM.

The oxidation peak current of D-Trp also linearly increases with increasing D-Trp concentrations in the range of 0.10–1.0 mM as shown in the inset of Fig. 3b. It is interesting to note that although the D- and L-enantiomers show increase in the current, the L-enantiomer gives higher current than the corresponding D-enantiomer at the ITO/APTES/GO/HSA electrode. This can be attributed to the enantioselective interaction between HSA and Trp prevents one enantiomeric form of Trp that is stronger than the other. This interpretation is in accordance with the fact that L-Trp has a stronger affinity to HSA than D-Trp does (Matsunaga et al., 2008). Due to Trp generally coexists in enantiomeric pairs in biological fluids and they show similar electrochemical behaviors at untreated carbon based electrodes, it is important to develop a rapid and simple method for the discrimination of one enantiomer in the presence of the other. In this manner, the ITO/APTES/GO/HSA electrode has been used for the simultaneous determination of D- and L-Trp.

Fig. 3c shows cyclic voltammograms of enantiomeric mixtures of Trp at different ratios of L- and D-Trp (1:0, 2:1, 1:1, 1:2 and 0:1, c/c). The oxidation potential of L-Trp shifts to the oxidation potential value of D-Trp along with the increasing amount of D-Trp. In addition, the oxidation of 1:1 (c/c) enantiomer mixture occurs approximately at 1.02 V. This potential value is mean of the oxidations of D- and L-Trp enantiomers indicating clearly that there is a racemic mixture in the medium. In this view, a linear calibration curve for the percentage of L-Trp is presented in the inset of Fig. 3c. This result indicates that the ITO/APTES/GO/HSA electrode gives an opportunity for not only enantiomeric discrimination of Trp pairs but also provides the determination of percentage of one enantiomer in a medium.

The stability of ITO/APTES/GO/HSA electrode was also evaluated by measuring the voltammetric current response of constant Trp concentration (0.1 mM) over a period of 10 days. It was observed that during the first 5 days the current response almost remained unchanged and showed a decrease in current density about 5% of its initial value at the end of the next 5 days.

4. Conclusion

The ITO/APTES/GO/HSA has been fabricated for discrimination of Trp enantiomers. The modified electrode is characterized by SEM, EIS and CV. The electrochemical discrimination of tryptophan enantiomers has been achieved. The graphene oxide layer

immobilized on the electrode surface has been expected not only for providing a large surface for stabilization of HSA at the electrode surface but also for separating the analytical signal occurring at the end of the interaction between HSA and D- or L-Trp. To the best of our knowledge, it is the first time to achieve chiral discrimination of tryptophan enantiomers electrochemically. When measurements applied to analyze D- and L-tryptophan mixture in a series of concentration, the percentage of an enantiomeric form has been successfully determined suggesting that this sensor can be used to analyze chiral mixtures. The ITO/APTES/GO/HSA electrode is very simple, cheap and not time consuming to produce and provide opportunity to make analysis for discrimination of D- and L-tryptophan. As a result, this study is expected to be a promising platform for discrimination of different chiral analytes by employing other chiral selectors.

Acknowledgment

The authors would like to thank S.U. Research Foundation (BAP) for financial support.

Appendix A. Supplementary material

Supplementary data associated with this article can be found in the online version at http://dx.doi.org/10.1016/j.bios.2012.10.068

References

Ahuja, T., Kumar, R.D., Tanwar, V.K., Sharma, V., Singh, N., Biradar, A.M., 2010. Thin Solid Films 519, 1128–1134.
Bu, Y., Wang, S., Chen, Q., Jin, H., Lin, J., Wang, J., 2012. Electrochemistry Communications 16, 80–83.
Chen, Q., Zhou, J., Han, Q., Wang, Y., Fu, Y., 2012. Colloids and Surfaces B: Biointerfaces 92, 130–135.
Girardet, C., Vardanega, D., Picaud, F., 2007. Chemical Physics Letters 443, 113–117.
Guo, Y., Guo, S., Fang, Y., Dong, S., 2010. Electrochimica Acta 55, 3927–3931.
Haak, R.M., Wezenberg, S.J., Kleij, A.W., 2010. Chemical Communications 46, 2713–2723.
Heli, H., Sattarahmady, N., Jabbari, A., Moosavi-Movahedi, A.A., Hakimelahi, G.H., Tsai, F.-Y., 2007. Journal of Electroanalytical Chemistry 610, 67–74.
Hummers, W.S., Offeman, R.E., 1958. Journal of the American Chemical Society 80, 1339.
Izake, E.L., 2007. Journal of Pharmaceutical Sciences 96, 1659–1676.
Jiang, Q., Sun, W., Jiao, K., 2010. Journal of Analytical Chemistry 65, 648–651.
Kim, C.O., Hong, S.-Y., Kim, M., Park, S.-M., Park, J.W., 2004. Journal of Colloid and Interface Science 277, 499–504.
Kumar, N.A., Choi, H.-J., Shin, Y.R., Chang, D.W., Dai, L., Baek, J.-B., 2012. ACS Nano 6, 1715–1723.
Liang, Y.-D., Song, J.-F., 2005. Journal of Pharmaceutical and Biomedical Analysis 38, 100–106.
Marcano, D.C., Kosynkin, D.V., Berlin, J.M., Sinitskii, A., Sun, Z., Slesarev, A., Alemany, L.B., Lu, W., Tour, J.M., 2010. ACS Nano 4, 4806–4814.
Matsunaga, M., Ueno, T., Nakanishi, T., Osaka, T., 2008. Electrochemistry Communications 10, 1844–1846.
Mazloum-Ardakani, M., Beitollahi, H., Taleat, Z., Naeimi, H., Taghavinia, N., 2010. Journal of Electroanalytical Chemistry 644, 1–6.
Miller, G.D., Johnson, J.A., Miller, B.S., 1956. Analytical Chemistry 28, 884–887.
Özcan, A., Sahin, Y., 2012. Biosensors & Bioelectronics 31, 26–31.
Prabhu, P., Babu, R.S., Narayanan, S.S., 2011. Colloids and Surfaces B: Biointerfaces 87, 103–108.
Raoof, J.-B., Ojani, R., Baghayeri, M., 2009. Sensors and Actuators B: Chemical 143, 261–269.
Simionato, A.V.C., Moraes, E.P., Carrilho, E., Tavares, M.F.M., Kenndler, E., 2008. Electrophoresis 29, 2051–2058.
Trojanowicz, M., Wcisło, M., 2005. Analytical Letters 38, 523–547.
Wang, Q., Das, M.R., Li, M., Boukherroub, R., Szunerits, S. Bioelectrochemistry (in press). http://dx.doi.org/10.1016/j.bioelechem.2012.03.004.
Wang, Z., Zhang, J., Chen, P., Zhou, X., Yang, Y., Wu, S., Niu, L., Han, Y., Wang, L., Chen, P., Boey, F., Zhang, Q., Liedberg, B., Zhang, H., 2011. Biosensors & Bioelectronics 26, 3881–3886.
Wang, Z., Zhou, X., Zhang, J., Boey, F., Zhang, H., 2009. Journal of Physical Chemistry C 113, 14071–14075.
Xu, C.-X., Huang, K.-J., Fan, Y., Wu, Z.-W., Li, J., Gan, T., 2012. Materials Science and Engineering C: Materials for Biological Applications 32, 969–974.
Xuan, W., Zhang, M., Liu, Y., Chen, Z., Cui, Y., 2012. Journal of the American Chemical Society 134, 6904–6907.
Zhao, Y., Pritts, W.A., Zhang, S., 2008. Journal of Chromatography A 1189, 245–253.
Zhen, Q., Xu, B., Ma, L., Tian, G., Tang, X., Ding, M., 2011. Clinical Biochemistry 44, 226–230.